ISSN-L 2664-9969; E-ISSN 2706-5448

UDC 66.081.63 + 544.77
DOI: 10.15587/2706-5448.2025.345312

**Liudmyla Bohdan,
Khrystyna Hutsul,
Olena Yanushevska,
Yurii Fedenko,
Tetiana Dontsova**

FEATURES OF OBTAINING SELECTIVE METAL OXIDE LAYERS FOR CERAMIC MEMBRANES VIA SOL-GEL METHOD

The object of research is metal oxide layers based on SiO_2, TiO_2, ZrO_2 for creating intermediate and selective layers on ceramic matrices. One of the most problematic areas is the difficulty of obtaining a uniform, dense, and stable selective layer determines the operational characteristics of the membrane – selectivity, productivity, and fouling resistance. The sol-gel method was used for synthesizing colloidal solutions of SiO_2, TiO_2, ZrO_2 and the spin-coating method for applying the resulting suspensions to ceramic matrices. The sizes of SiO_2, TiO_2, ZrO_2 particles were determined by turbidimetry, with diameters of 159 nm, 79 nm, and 99 nm, respectively. The results of IR spectroscopy show that the application of TiO_2 selective layer by spin-coating allows for complete coverage of the membrane surface, while the application of ZrO_2 layer results in incomplete coverage with confirmation of the formation of a hydrated precipitate. Studies of morphology by scanning electron microscopy indicate a coarse-grained matrix structure and a more homogeneous medium-grained structure after applying an intermediate SiO_2 layer. The transport properties of ceramic matrices and membranes were determined by their permeability to pure water indicates high permeability of both matrices and membranes. Thus, the sol-gel method in combination with spin-coating has several features, in particular, controlled hydrolysis of precursors and the possibility of step-by-step formation of uniform layers makes it possible to obtain membranes with high water permeability (over 560 cm^3/min) and a stable microfiltration structure after applying only 5 layers. Compared to similar methods, the proposed approach provides uniform coverage, less particle agglomeration, increased process reproducibility, enabling the creation of ceramic microfiltration membranes for water purification processes.

Keywords: *selective layers, metal oxides, spin-coating, ceramic membranes, sol-gel method, water permeability.*

Received: 03.09.2025
Received in revised form: 09.11.2025
Accepted: 01.12.2025
Published: 29.12.2025

How to cite
Bohdan, L., Hutsul, K., Yanushevska, O., Fedenko, Y., Dontsova, T. (2025). Features of obtaining selective metal oxide layers for ceramic membranes via sol-gel method. Technology Audit and Production Reserves, 6 (3 (86)), 12–20. https://doi.org/10.15587/2706-5448.2025.345312

1. Introduction

Ceramic membranes with selective layers based on metal oxides are used in many industries, for purifying solutions and separating suspensions [1]. The use of ceramic membranes is particularly justified in the purification of oil-containing waters due to their more hydrophilic surface compared to their polymer counterparts [2]. The hydrophilicity of ceramic membranes is due to the presence of hydroxyl (–OH) groups on their surface, the density of which is significantly reduced after high-temperature sintering of ceramics in membrane manufacturing technology [3].

The sol-gel method is widely used for synthesizing nanoparticles of various chemical compositions, which are widely used particularly for the synthesis of metal oxides at moderate temperatures and pressures. The sol-gel method is also actively used for the synthesis of selective layers based on silicon (IV) oxide (SiO_2) [4], titanium (IV) oxide (TiO_2) [5], and zirconium (IV) oxide (ZrO_2) [6]. It should be noted that TiO_2 and ZrO_2 are highly chemically stable in acidic and basic environments, which makes them particularly attractive for the creation of selective layers of ceramic membranes [1].

It is known that various precursors can be used for sol-gel synthesis, which makes it possible to control the microstructure of the selective membrane layer and influence its surface characteristics. Sol-solutions are usually applied to the membrane matrix either by dip-coating or spin-coating, the purpose of which is to reduce the size of the membrane pores, resulting in certain selective properties of the membranes [7].

There are many examples in the literature of obtaining thin films of various thicknesses from millimeter-thick layers of sol-gel solutions. For example, in [8], silica (SiO_2) nanoparticles with different concentrations were applied to the surface of commercial ceramic TiO_2 membranes using dip-coating. This made it possible to improve the properties of existing ceramic membranes, namely, to significantly increase their hydrophilicity, which, in turn, improved their transport properties.

Thin TiO_2 films were obtained using the sol-gel method with titanium (IV) tetraisopropoxide (TTIP) as a precursor, ethanol as a solvent, and acetylacetone as a stabilizer [9]. The prepared mixture was repeatedly applied to the substrates by injection and evenly distributed on the substrate by centrifugation to form a multilayer film. The results of X-ray diffraction analysis confirmed that TiO_2 in the formed films has an anatase structure, and the size of TiO_2 crystallites varies depending on the number of layers in the range of 16–19 nm. It was proven that the number of layers of applied TiO_2 films affects their properties, such as optical, electrical, photocatalytic, and antibacterial, which confirms the possibility of technological application of such multilayer films in technologies for creating sensor and photocatalytic coatings using physicochemical research methods [10]. Similar studies leading to the production of nanoscale and nanocrystalline TiO_2 are reflected in many scientific studies, for example [11].

Research [12] has shown the possibility of using the sol-gel method to obtain nanocomposite thin films of TiO_2 with manganese. The sol was prepared from titanium tetraisopropoxide, isopropyl alcohol (99.5%), and the addition of nitric acid solution. The Mn dopant was added in the form of a manganese (II) acetate tetrahydrate solution. The resulting sol was applied to a cleaned glass substrate by centrifuging six layers at regular intervals to achieve the desired final layer thickness of approximately 350 nm.

There are known works where zinc [13], chromium [14], calcium and manganese [15], platinum [16] served as doping additives to TiO_2 sols for the creation of thin layers. The effect of cobalt ion doping on the nanostructure, optical, electronic, photoluminescent, and magnetic properties of $Zr_1–Co_xO_2$ films with a thickness of 115 to 70 nm synthesized by the sol-gel method was investigated [17]. The study [18] presented an overview of the latest achievements in the creation of $TiO_2–ZrO_2$ composite coatings obtained by the sol-gel method with the addition of polymers, which led to the formation of homogeneous integral films with improved adhesive properties, significant antibacterial and photocatalytic activity, making them promise for medical applications, water and air purification. The use of the sol-gel method in [19] for the synthesis of ZnO/TiO_2 nanocomposites also proves that the obtained materials have antibacterial and photocatalytic properties, and studies [20] showed the ability of CuO/TiO_2 hybrid nanostructures synthesized by the sol-gel method to exhibit photocatalytic activity in the degradation of P-nitrophenol (PNP) in industrial wastewater under the influence of solar radiation.

It is interesting to note that the sol-gel method is rarely used for the synthesis of ZrO_2 nanoparticles [21]. In general, the sol-gel method is used for the synthesis of ZrO_2 nanoparticles, where the focus is on studying the resulting modification, the degree of crystallinity, and the size and morphology of the nanoparticles [22].

Also, membrane fouling is one of the challenges in technologies for purifying water from petroleum products. It leads to higher energy consumption and a reduction in their service life. The introduction of various methods for modifying ceramic membranes to increase their operational efficiency is discussed in [23]. The sol-gel method remains a widely used strategy for modifying ceramic membranes, which is used to create thin selective layers with controlled porosity. An example of the creation of nanofiltration membranes with a TiO_2-based coating is given in [24]. The properties of the selective layer of ceramic microfiltration membranes based on Al_2O_3, TiO_2, or ZrO_2 (nominal pore size 0.1 μm) were studied in the processes of milk protein fractionation [25]. The thickness of the selective layer of the membranes consisted of six layers, and the filtration efficiency during milk protein fractionation was studied at different transmembrane pressures and temperatures. The positive effect of the sol-gel technology use on filtration efficiency and reduction of membrane fouling was demonstrated.

This article discusses the peculiarities of synthesizing selective metal oxide layers using the sol-gel method to create ceramic membranes, which is currently a controversial issue in scientific literature.

The object of research is metal oxide layers based on SiO_2, TiO_2, and ZrO_2 for the creation of intermediate and selective layers on ceramic matrices.

Thus, *the aim of research* is to identify the features of obtaining selective metal oxide layers (SiO_2, TiO_2, and ZrO_2) for ceramic membranes using the sol-gel method and to study their physicochemical properties.

Therefore, *the tasks of research* are:

1. Investigate the kinetics of SiO_2, TiO_2 and ZrO_2 particle formation by hydrolysis and determine particle size by turbidimetry.
2. Characterize the obtained intermediate and selective layers using IR spectroscopy.
3. Investigate the morphology of matrices, intermediate and selective layers using scanning electron microscopy.
4. Establish the transport properties of synthesized ceramic matrices and membranes in order to determine their application in membrane technologies.

2. Materials and Methods

SiC-based ceramic matrices were used to apply selective layers. These matrices were manufactured using dry pressing, the characteristics and composition of which are described in [26]. Colloidal solutions of SiO_2, TiO_2, and ZrO_2 were synthesized as follows:

SiO_2: 3 cm^3 of tetraethyl orthosilicate ($Si(OC_2H_5)_4$) solution was dissolved in 6 cm^3 of isopropyl alcohol (C_3H_7OH) with constant stirring, 3 cm^3 of distilled water was added to the solution and the pH of the mixture was adjusted to pH 2 by adding nitric acid with a concentration of 3 mol/dm^3. The solution was heated for 10 min at temperature of 80°C (Fig. 1, *a*).

TiO_2: 2 cm^3 of triethanolamine ($C_6H_{15}NO_3$) was added to 10 cm^3 of isopropyl alcohol (C_3H_7OH) with constant stirring, 3.5 cm^3 of titanium (IV) isopropoxide ($C_{12}H_{28}O_4Ti$) and 1 cm^3 of distilled water were added dropwise to initiate the hydrolysis process and stirred for 10 minutes on a magnetic stirrer (Fig. 1, *b*).

ZrO_2: 10 g of zirconium (IV) oxychloride ($ZrOCl_2 \cdot 8H_2O$) was added to 80 cm^3 of distilled water, and the mixture was subjected to ultrasonic treatment to completely dissolve $ZrOCl_2 \cdot 8H_2O$.

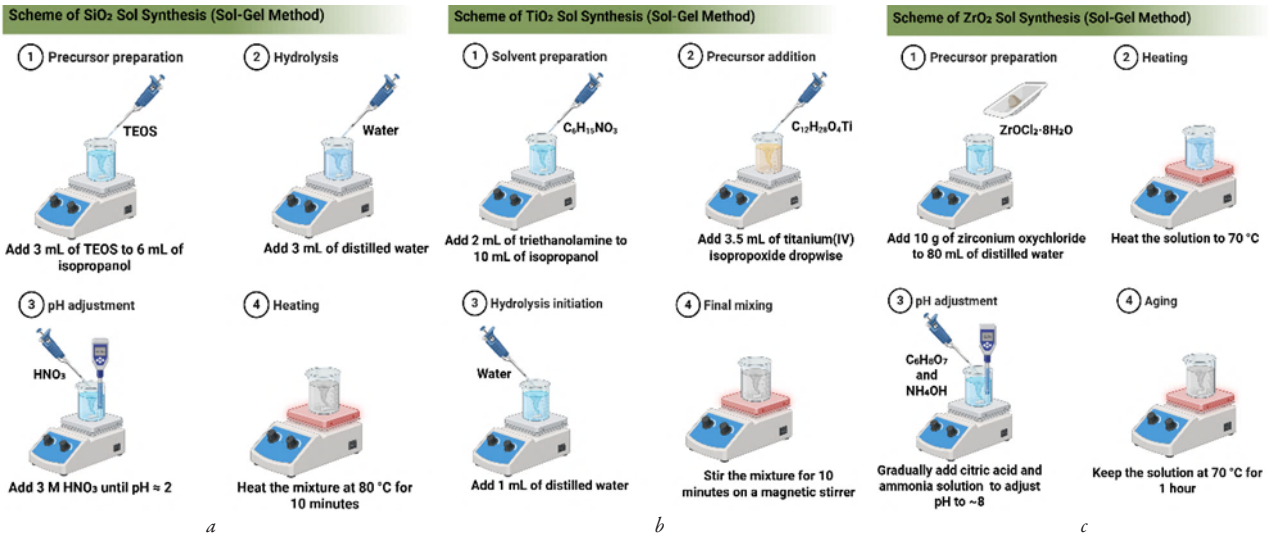

a *b* *c*

Fig. 1. Schemes for the synthesis of metal oxides colloidal solutions:
a – scheme of SiO_2 sol synthesis; *b* – scheme of TiO_2 sol synthesis; *c* – scheme of ZrO_2 sol synthesis

ISSN-L 2664-9969; E-ISSN 2706-5448

Next, the solution was heated on a magnetic stirrer to 70°C, gradually adding citric acid ($C_6H_8O_7$) and ammonia water (NH_4OH) to adjust the pH to 8. The resulting solution was kept at 70°C for another hour (Fig. 1, *c*).

The kinetics of colloidal solution formation were studied using spectrophotometry (Shimadzu, UV-2600, Japan). The solutions prepared as described above were transferred to cuvettes and placed in the spectrophotometer cell, and the absorption spectrum was recorded at wavelengths from 200 nm to 500 nm: starting from 20 seconds at a frequency of once per minute for the SiO_2 suspension; starting from 10 seconds at 30-second intervals for the TiO_2 suspension; before and after adding the precipitant for the ZrO_2 suspension. In all cases, isopropyl alcohol solution served as the reference solution.

The turbidimetry method was used to determine the particle sizes of metal oxides (SiO_2, TiO_2, and ZrO_2). For this purpose, powders obtained by the sol-gel method and pre-dried and calcined at 500°C were dispersed in distilled water with subsequent ultrasonic treatment to prevent particle aggregation, preparing "white sols" of the specified oxides with concentrations of 10, 30, 50, and 70 g/dm^3. An inSpect-101UV spectrophotometer (190–1000 nm, Spectrometer 65TM, China) was used to determine the optical density range for each suspension at wavelength of 400 nm (Fig. 2).

Samples of suspensions with optical density ranging from 0.7 to 0.95 were considered as working suspensions for determining the particle size in them according to the method described in [27].

The surface of ceramic matrices and matrices with intermediate and selective layers (membranes) was studied using IR Fourier spectroscopy (Shimadzu, IRXross FTIR spectrophotometer, Japan) in the range of 10,000–100 cm^{-1}.

SEM images of samples of the obtained selective layers and matrices were obtained using a Quanta Inspect – SEM Tungsten microscope from Thermo FEI, 30.0 kV, magnification range 1.3 kx–177 kx.

The spin-coating method was used to obtain intermediate (SiO_2) and selective (TiO_2 and ZrO_2) layers on ceramic matrices. This method consisted of the following. Synthesized suspensions with a volume of 0.2 cm^3 were injected into a flat round ceramic matrix, placed in a centrifuge, and rapidly rotated for 15 seconds (1000 rpm). The matrix was dried at 80°C for 30 minutes after applying each layer, and after the applied layer had dried, the next layer was applied using the same method and dried again. In this way, a specified number of intermediate and selective layers were applied (Table 1). The dried layers were then fired in an oven for 1 hour at a temperature of 550°C.

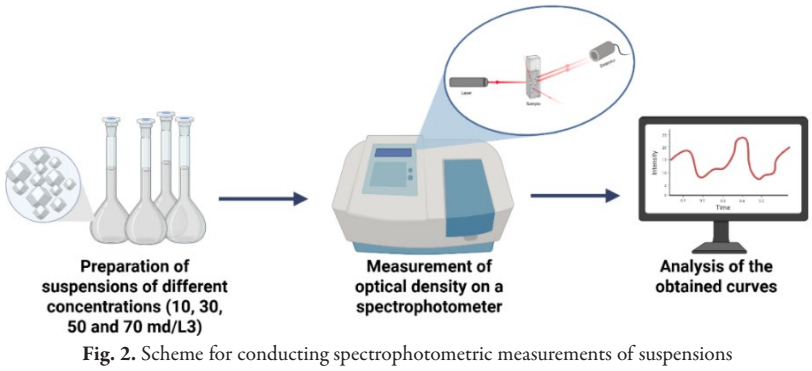

Fig. 2. Scheme for conducting spectrophotometric measurements of suspensions

Table 1

Ceramic matrices obtained with applied layers

Sample	Number of intermediate layers based on SiO_2	Number of selective layers	
		Based on TiO_2	Based on ZrO_2
S3	3	–	–
S3T3	3	3	–
S3T5	3	5	–
S3T7	3	7	–
S3Z5	3	–	5

The water permeability of ceramic matrix and membrane samples was determined in a special cell printed on a 3D printer (Anycubic Photon Mono M5s DLP 3D printer, China) [28]. The matrix samples with applied layers were pretreated before starting the tests: they were sequentially washed with distilled water and ethanol in an ultrasonic bath for 5 minutes, after which they were dried in a drying oven. Next, the membranes washed in this way were placed in a cell, to which water was supplied using a pump, and the volume of water passing through the membrane in 1 minute was measured. The pressure on the manometer was also recorded during the passage of the flow through the membrane.

3. Results and Discussion

3.1. Study of kinetics of sol formation based on SiO_2, TiO_2, and ZrO_2 and determination of sol particle sizes

The results of kinetic studies of sol formation based on SiO_2, TiO_2, and ZrO_2 are presented in Fig. 3.

The intensity of the kinetic curve's peaks for SiO_2 gradually increases with an increase in the duration of tetraethyl orthosilicate hydrolysis, and the peaks themselves shift towards higher wavelength values, indicating an increase in the number and size of the SiO_2 particles formed, as can be seen from Fig. 3. The process of TiO_2 particle formation occurs faster than the formation of SiO_2 particles due to the hydrolysis of titanium (IV) isopropoxide – the formation of a larger number of TiO_2 particles occurred within the first 10 seconds (curve – 1). The shape of the other curves indicates possible particle agglomeration. It was impossible to study the kinetics of ZrO_2 particle formation in solution because the hydrolysis reaction does not occur without the addition of ammonia water, and after its addition, the reaction occurs instantly with the simultaneous formation of a precipitate, probably $ZrO_2 \cdot H_2O$. Therefore, in this case, two spectra were recorded: for the initial solution of zirconium (IV) oxychloride and for the ZrO_2 suspension obtained after the addition of ammonia water (pH 8).

A literature review was additionally conducted on the chemistry involved in these cases to understand the processes occurring during synthesis. It is known [29] that the process of forming nanoscale silicon (IV) oxide involves the following sequential stages: hydrolysis of tetraethyl orthosilicate ($Si(OC_2H_5)_4$) with the formation of silanol groups and condensation polymerization between silanol groups and ethoxy groups with the formation of siloxane bonds, which, through a polymerization reaction, form three-dimensional SiO_2 structures, which can be schematically represented as follows:

$$Si{-}(OC_2H_5)_4 + H_2O \times Si{-}(OH)_4 + 4R{-}OH,$$

$$2Si{-}(OH)_4 \rightarrow 2(Si{-}O{-}Si) + 4H_2O.$$

The process of forming titanium (IV) oxide nanoparticles using the sol-gel method and titanium alkoxide ($C_{12}H_{28}O_4Ti$) as a titanium precursor includes the stages of hydrolysis and gel formation, which involves the formation of a three-dimensional TiO_2 structure through Ti–O–Ti bonds [30]. The stages of condensation (dehydration and dealkylation) proceed almost in parallel after the initiation of hydrolysis, which occurs gradually, and are schematically described by the equations:

$$M(OR)_n + H_2O \rightarrow M(OR)_{n-1}(OH) + ROH,$$

$$2M(OR)_{n-1}(OH) \leftrightarrow M_2O(OR)_{2n-2} + H_2O,$$

$$M(OR)_n + M(OR)_{n-1} \rightarrow M_2O(OR)_{2n-2} + ROH.$$

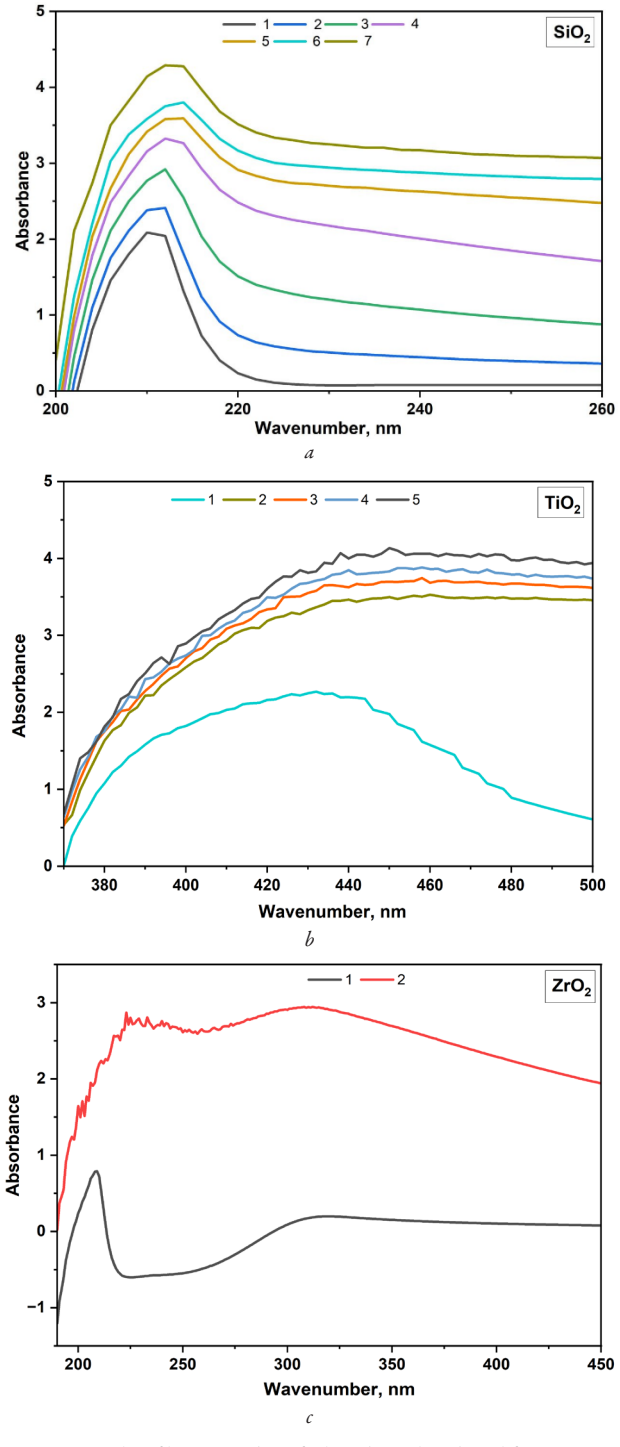

Fig. 3. Results of kinetic studies of selected metal oxides sol formation: *a* – kinetic studies of SiO_2: 1 – SiO_2 sol after 20 seconds after stirring, 2, 3, 4, 5, 6, 7 – SiO_2 sol after every 60 seconds, respectively; *b* – kinetic studies of TiO_2: 1 – TiO_2 sol after 10 seconds after stirring, 2, 3, 4, 5 – TiO_2 sol after every 30 seconds, respectively; *c* – kinetic studies of ZrO_2: 1 – initial solution before adding ammonia water, 2 – $ZrO_2 \cdot H_2O$ suspension after adding ammonia water

The hydrolysis reaction of zirconium (IV) oxochloride octahydrate ($ZrOCl_2 \cdot 8H_2O$) occurs with the destruction of Zr–Cl bonds and the formation of $ZrO_2 \cdot H_2O$ and, accordingly, Zr–OH bonds, as described in [31]. Subsequently, Zr–O–Zr bonds are formed through condensation polymerization between Zr–OH groups, and water molecules are released, leading to the formation of a colloidal solution of zirconium (IV) oxide. At the same time, the process of ZrO_2 particle formation, as shown in [32], occurs only when the aqueous solution of $ZrOCl_2 \cdot 8H_2O$ is heated, during which both the dehydration of the octahydrate and its hydrolysis can occur simultaneously, with the rate of these reactions being determined by the temperature. In simplified terms, the chemistry of these processes will proceed according to the following reaction

$$ZrOCl_2 \cdot 8H_2O \leftrightarrow ZrO_2 \cdot nH_2O + 2HCl + (8 - n)H_2O.$$

Thus, the experimental results obtained and the literature data presented are fully consistent with each other.

The results of determining the optical density of SiO_2, TiO_2, and ZrO_2 suspensions are presented in Table 2. As can be seen, the optical density is within the desired range, namely 0.7–0.95, for SiO_2 and TiO_2 suspensions at a concentration of 70 mg/dm^3, and for ZrO_2 suspension at 50 mg/dm^3. Therefore, these concentrations were chosen to determine the particle sizes of the corresponding oxides.

Table 2

Optical density of SiO_2, TiO_2, and ZrO_2 suspensions as a function of concentration at a wavelength 400 nm

Concentration	Optical density		
	SiO_2	TiO_2	ZrO_2
10 mg/dm^3	0.074	0.045	0.095
30 mg/dm^3	0.406	0.185	0.366
50 mg/dm^3	0.693	0.573	0.874
70 mg/dm^3	0.924	0.868	1.211

Next, absorption spectra were recorded in the wavelength range of 200–1000 nm (Fig. 4) for selected concentrations of oxides in suspensions, and logarithms were taken for optical density values in the 400–600 nm range (Table 3), and, based on the results obtained, the dependence of lg$D$ on lgλ was plotted (Fig. 5).

The degree n was calculated based on the logarithmic dependencies obtained, and was 2.349 for SiO_2, 3.095 for TiO_2, and 2.824 for ZrO_2, and the values of the Z coefficient were determined, which were 8, 4, and 5 for SiO_2, TiO_2, and ZrO_2 suspensions, respectively.

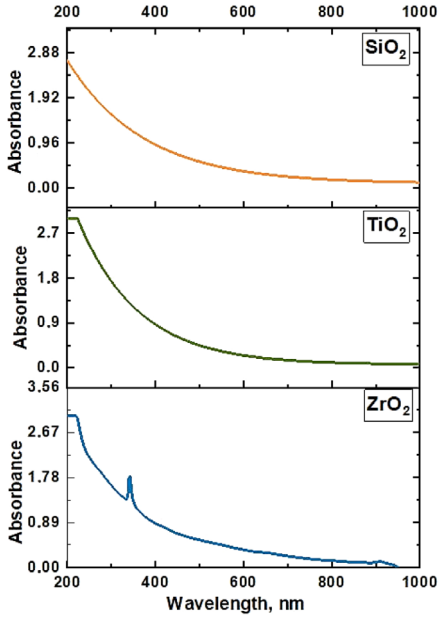

Fig. 4. Absorption spectra of SiO_2 (70 mg/dm^3), TiO_2 (70 mg/dm^3), and ZrO_2 (50 mg/dm^3) suspensions

ISSN-L 2664-9969; E-ISSN 2706-5448

Table 3

Optical density values in the 400–600 nm range of SiO_2, TiO_2, and ZrO_2 suspensions

Wavelength, nm	Optical density		
	SiO_2 (C = 70 mg/dm^3)	TiO_2 (C = 70 mg/dm^3)	ZrO_2 (C = 50 mg/dm^3)
400	0.924	0.868	0.874
450	0.710	0.616	0.645
500	0.563	0.451	0.478
550	0.447	0.335	0.369
600	0.354	0.245	0.276

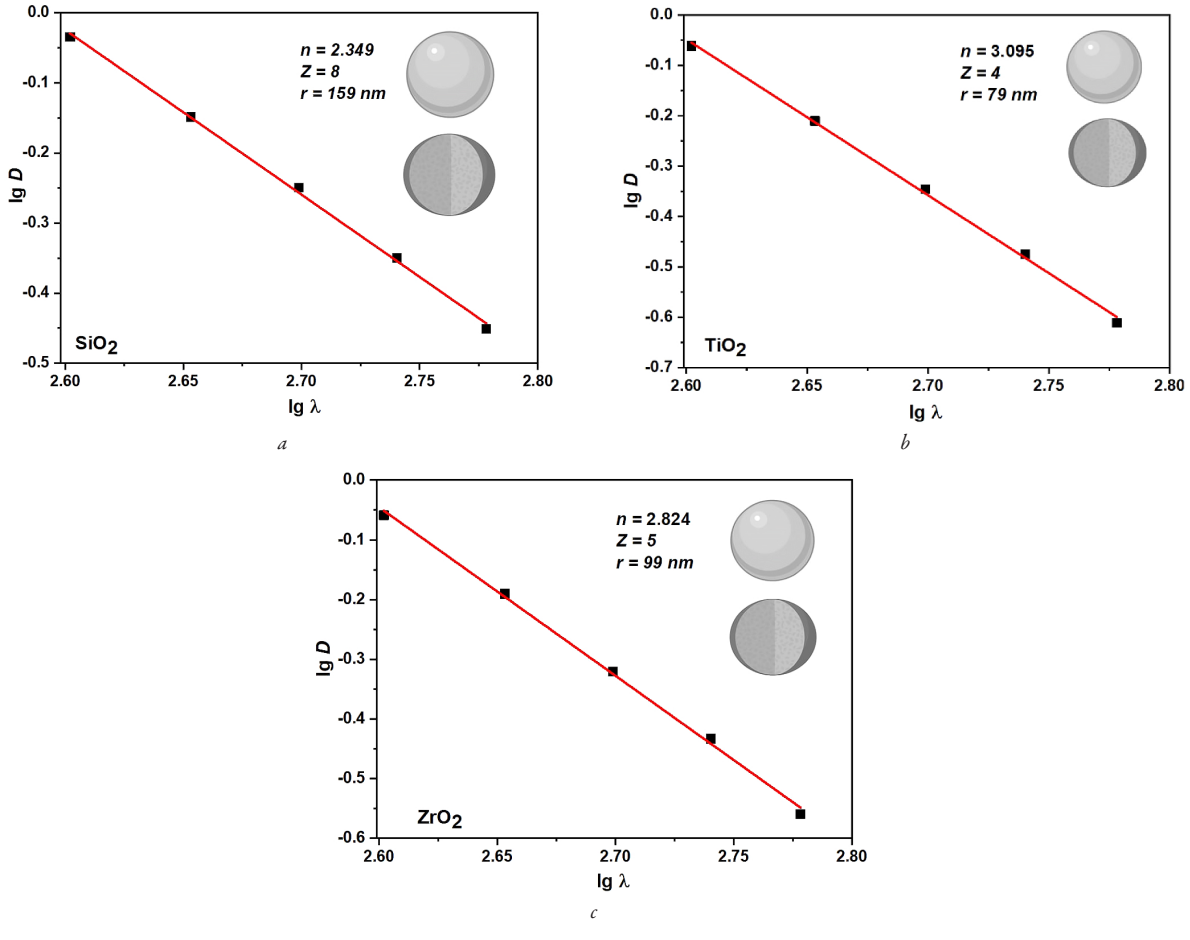

Fig. 5. Logarithmic dependencies of optical density values in the 400–600 nm range for suspensions of: *a* – SiO_2 (70 mg/dm^3); *b* – TiO_2 (70 mg/dm^3); *c* – ZrO_2 (50 mg/dm^3)

The diameter of SiO_2, TiO_2, and ZrO_2 particles was calculated using the Heller equation and based on the obtained Z values, and was 159 nm, 79 nm, and 99 nm, respectively.

3.2. Infrared spectra of ceramic matrix and membrane samples

IR Fourier spectroscopy was used to study the surface of ceramic matrices, matrices with applied intermediate layers (SiO_2) and intermediate (SiO_2) selective layers (TiO_2, ZrO_2) simultaneously to confirm that an intermediate layer had formed on the surface of the ceramic matrix. Fig. 6 shows the corresponding IR spectra.

The spectrum of the ceramic matrix (Fig. 6, *a*) shows peaks in the range of 400–500 cm^{-1}, corresponding to Si–O bond vibrations; 615 cm^{-1} corresponds to Si–Si bond vibrations, and 787 and 850 correspond to Si–C [33]. The peak at 1100 cm^{-1} can be attributed to Si–O–Si and/or Si–O–C bond vibrations according to [2], which indicates the chemical bonding of the matrix components.

The presence of peaks in the IR spectrum of sample S3 (Fig. 6, *b*) in the range of 400–470 cm^{-1} indicates vibrations of Si–O bonds, and at 780 cm^{-1} – Si–C bonds [33]. The peak at 1100 cm^{-1} corresponds to the vibrations of Si–O–Si and/or Si–O–C bonds [34], which also indicates the chemical bonding of the intermediate layer with the ceramic matrix.

The IR spectrum of sample S3T5 (Fig. 6, *c*) shows peaks only in the 400–500 cm^{-1} range, corresponding to the frequency of vibrations of both Ti–O [35], and Ti–O–Ti [36], bonds, which may indicate complete coverage of the matrix and selective layer with titanium (IV) oxide.

Sample S3Z5 (Fig. 6, *d*) is characterized by peaks in the 400–500 cm^{-1} and 500–800 cm^{-1} regions, which belong to Zr–O and Zr–O–Zr vibrations, respectively [37]. The presence of peaks at 1600 cm^{-1} and 3200–3600 cm^{-1} confirms the formation of $ZrO_2 \cdot H_2O$ precipitate, which was observed in kinetic studies, since these peaks correspond to Zr–OH and OH vibrations in physically bound water, respectively [37]. The presence of a peak in the IR spectrum of S3Z5 at 1100 cm^{-1} indicates incomplete coverage of the membrane with a selective layer based on ZrO_2, corresponding to Si–O–Si vibrations [34] of the intermediate layer.

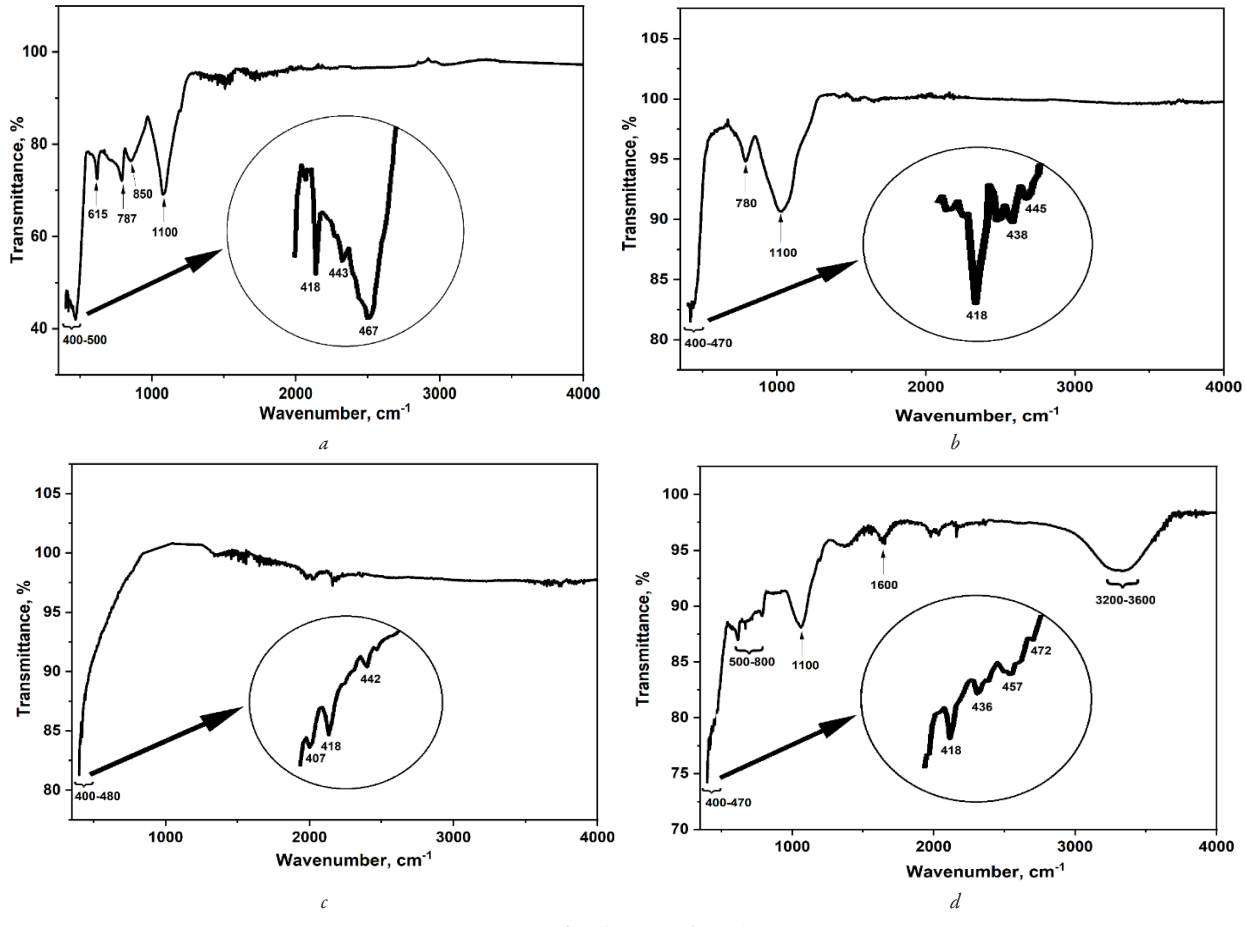

a *b* *c* *d*

Fig. 6. Infrared spectra of samples:
a – ceramic matrix; *b* – sample S3; *c* – sample S3T5; *d* – sample S3Z5

3.3. Scanning electron microscopy images of ceramic matrices with applied layers

The ceramic matrix has a granular structure with grain sizes of 10 μm (Fig. 7, *a*).

Coating with an intermediate layer changes the structure from coarse-grained to medium-grained (Fig. 7, *b*).

Further application of selective layers results in a homogeneous surface structure in the case of both titanium (IV) oxide (Fig. 7, *c*) and zirconium (IV) oxide (Fig. 7, *d*), with a difference in the size of their pores.

Fig. 7 shows SEM images of the ceramic matrix, sample S3, and samples with selective layers S3T5 and S3Z5.

3.4. Investigation of transport properties of ceramic matrices and membranes

The transport properties of ceramic matrices and membranes were determined by their permeability to pure water. The results of measuring the permeability of the obtained ceramic matrices and membranes to pure water are presented in Table 4.

The throughput capacity for ceramic matrices is 560–598 cm^3/min, as can be seen from Table 4.

At the same time, no pressure increase was observed when water passed through the ceramic matrices. The data obtained are quite positive, since the matrices must have a high capacity for throat under normal conditions.

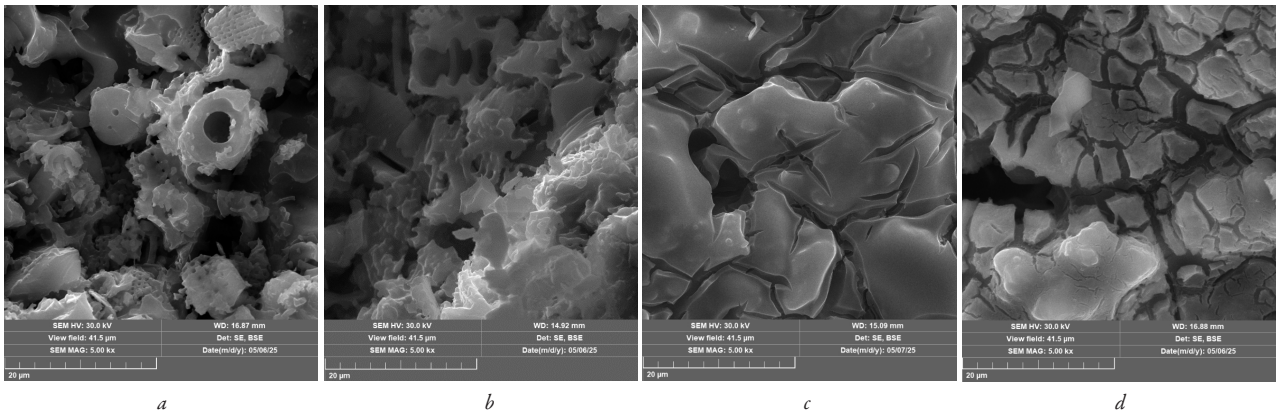

a *b* *c* *d*

Fig. 7. Scanning electron microscopy images of ceramic matrix and membrane samples:
a – ceramic matrix; *b* – sample S3; *c* – sample S3T5; *d* – sample S3Z5

ISSN-L 2664-9969; E-ISSN 2706-5448

Table 4

Clean water permeability of ceramic matrices obtained with coating

No.	Volume of water passing through the membrane per minute, cm^3					
	Ceramic matrix	S3	S3T3	S3T5	S3T7	S3Z5
1	598	564	472	–	–	–
2	560	525	–	360	–	–
3	580	555	–	–	392	–
4	598	568	–	–	–	420

Applying an intermediate layer to the matrices leads to a 4–6% decrease in flow capacity, for which no pressure was observed either, i. e., it was zero. The throughput decreased after applying selective layers with TiO_2 and ZrO_2: for the S3T3 membrane by 16.3%; for the S3T5 membrane by 31.4%, for the S3T7 membrane by 29.4%; for the S3Z5 membrane by 26%. At the same time, an increase in pressure to 1.5 bar was observed for the S3T3 membrane, and to 2 bar for the other membranes.

Thus, the use of the sol-gel method for obtaining selective layers and the spin-coating method for applying them to ceramic matrices allows obtaining microfiltration membranes where 5 layers may already be sufficient.

3.5. Discussion

Analysis of the kinetic curves in Fig. 3 and absorption spectra in Fig. 4, forming the basis for calculations using the Heller equation, namely, obtaining logarithmic dependencies of optical density values on wavelength in the range 400–600 nm (Fig. 5) confirms the existing understanding of the process of SiO_2 formation (Fig. 3, *a*), TiO_2 (Fig. 3, *b*), and ZrO_2 (Fig. 3, *c*) sols/suspensions. Thus, the formation of SiO_2 particles, including the successive stages of hydrolysis of tetraethyl orthosilicate ($Si(OC_2H_5)_4$) with the formation of silanol groups, condensation polymerization with the formation of siloxane bonds, and polymerization reaction with the formation of three-dimensional SiO_2 structures, leads to the formation of larger particles, which is 159 nm. This size of SiO_2 sol particles and their relatively slow sedimentation rate may be recommended for the synthesis of an intermediate layer sol for application to ceramic microfiltration matrices by spin-coating.

In contrast, the process of TiO_2 particle formation occurs faster (within the first 10 seconds, Fig. 3, *b*, curve – 1) due to the hydrolysis of titanium (IV) isopropoxide ($C_{12}H_{28}O_4Ti$) with the formation of a larger number of TiO_2 particle nuclei, leading to the formation of a larger number of finer particles (79 nm). The stages of condensation, namely dehydration and dealkylation, proceed almost in parallel after the start of hydrolysis and do not lead to significant agglomeration of nanoparticles. It should be noted that the nanoscale sol, from which TiO_2 was formed, is desirable for creating a selective membrane layer, which will determine its selectivity with respect to pollutants by size.

At the same time, it has been found that the hydrolysis reaction of $ZrOCl_2 \cdot 8H_2O$ does not occur without the addition of ammonia water, and after its addition, a precipitate is instantly formed, probably of hydrated zirconium (IV) oxide (Fig. 3, *c*, curve – 2), which correlates with classical ideas based on the analysis of scientific literature. It is believed that the hydrolysis reaction occurs due to the destruction of Zr–Cl bonds with the formation of Zr–OH and subsequent condensation polymerization between Zr–OH groups with the formation of Zr–O–Zr, and after the release of water molecules, to the formation of hydrated colloidal particles of zirconium (IV) oxide. Such particles quickly aggregate with each other and form a precipitation that is not suitable for application to ceramic matrices.

The results of the IR spectrum analysis of sample S3 (Fig. 6, *b*) with an intermediate layer of SiO_2 applied by spin-coating indicate the presence of a chemical bond (Si–O–C) between the intermediate layer and the ceramic matrix, which indicates good adhesion between the layers. The IR spectrum of sample S3T5 (Fig. 6, *c*) demonstrates the uniformity of the titanium (IV) oxide sol coating of the ceramic matrix with an intermediate layer. This indicates the possibility of using the proposed spin-coating method to apply a selective layer of TiO_2 nanoparticles formed by the sol-gel method to the surface layer of ceramic matrices. However, IR analysis of sample S3Z5 showed that the selective layer based on ZrO_2 does not form a uniform coating, as evidenced by the presence of uncovered areas of the intermediate layer surface (the presence of a peak at 1100 cm^{-1} in Fig. 6, *d*, corresponding to Si–O–Si bonds). The spectrum also has peaks at 1600 cm^{-1} and 3200–3600 cm^{-1}, indicating the formation of $ZrO_2 \cdot H_2O$ precipitation and confirms the results of kinetic studies.

SEM images demonstrate the possibility of using SiO_2 sols and the spin-coating method to form intermediate layers for preparing ceramic membranes for the application of selective layers by leveling the surface of ceramic matrices and narrowing the pores (Fig. 7, *b*). As a result, the selective layer based on titanium (IV) oxide (Fig. 7, *c*) has a homogeneous structure and is evenly distributed over the membrane surface. The layer based on zirconium (IV) oxide (Fig. 7, *d*) also has a homogeneous morphology of individual areas of the applied layer (albeit with larger pores), but there are violations of the integrity of the application due to its cracking.

The decrease in permeability (Table 4) and the increase in working pressure to 2 bars during water passage through membrane samples with selective layers applied to the intermediate layer indicate a decrease in pores compared to the ceramic matrix and intermediate layer. It may also indicate the possibility of creating a selective layer synthesized by the sol-gel method, strong adhesion of layers on the surface of the ceramic membrane, and the possibility of using such ceramic membranes for microfiltration processes.

The practical significance of research: the results obtained may be useful for improving the manufacturing process of ceramic microfiltration membranes for use in membrane technologies.

Limitations of research: the results obtained in research require further research in order to improve the method of applying intermediate and selective layers to obtain strong layers on the surface of matrices, as well as testing the obtained membranes in real conditions.

Prospects for further research: further research may be devoted to determining the effect of various parameters of applying an intermediate layer based on SiO_2 and a selective layer of TiO_2 to ceramic matrices to obtain microfiltration and nanofiltration membranes with different selectivity.

4. Conclusions

1. Kinetic studies on the oxide particles formation show that the synthesis of SiO_2 and TiO_2 particles occur because of hydrolysis, while ZrO_2 is obtained only after adding alkali to its solution, which leads to the formation of a highly hydrated precipitate. The sizes of SiO_2, TiO_2, and ZrO_2 particles were determined to be 159 nm, 79 nm, and 99 nm, respectively, based on the obtained absorption spectra and using the turbidimetry method, and which indicates the promise of the sol-gel method for the synthesis of intermediate and selective layers.

2. R spectroscopy showed that the application of a selective layer based on titanium (IV) oxide by spin-coating allows complete coverage of the matrix and intermediate layer, while the IR spectrum of the zirconium (IV) oxide-based layer indicates incomplete coverage with confirmation of the formation of a strongly hydrated precipitate – $ZrO_2 \cdot H_2O$.

3. The SEM images of the morphology obtained in the work indicate a coarse-grained structure of the matrix and a more homogeneous

medium-grained structure after applying the intermediate layer of SiO_2. The application of selective layers (TiO_2 and ZrO_2) leads to the formation of even more homogeneous structures, which differ in the size of the pores in them.

4. It has been established that the transport properties of ceramic matrices and membranes, determined by their permeability to pure water, indicate a high permeability of all matrices and membranes, but an increase in pressure to 2 bar was observed after applying selective layers based on both TiO_2 and ZrO_2 using the spin-coating method, indicating the production of microfiltration membranes.

Conflict of interest

The authors declare that they have no conflict of interest in relation to this research, including financial, personal, authorship or other, which could affect the research and its results presented in this article.

Financing

National Research Foundation of Ukraine for funding the project "Scientific Basis of Synthesis of Advanced Ceramic Membranes Using 3D Printing Technologies" (project registration number 2023.03/0178), Ministry of Education and Science of Ukraine for funding the applied research project "Chemically Modified Membranes for Rapid Detection of Nitrogen Compounds in Natural Waters as Markers of Explosives" (state registration number 0124U001095).

Data availability

The manuscript has no associated data.

Use of artificial intelligence

The authors confirm that they did not use artificial intelligence technologies when creating the presented work.

Acknowledgments

We are grateful to the National Research Foundation of Ukraine for funding the project "Scientific Basis of Synthesis of Advanced Ceramic Membranes Using 3D Printing Technologies" (project registration number 2023.03/0178 within the framework of the 2023.03 competition "Advanced Science in Ukraine") and the Ministry of Education and Science of Ukraine for funding the applied research project "Chemically Modified Membranes for Rapid Detection of Nitrogen Compounds in Natural Waters as Markers of Explosives" (state registration number 0124U001095).

Authors' contributions

Liudmyla Bohdan: Investigation, Validation, Data curation, Visualization, Writing – original draft, Writing – review and editing; ***Khrystyna Hutsul***: Investigation, Validation, Data curation, Visualization, Writing – original draft; ***Olena Yanushevska***: Conceptualization, Formal analysis, Writing – review and editing; ***Yurii Fedenko***: Writing – original draft, Writing – review and editing; ***Tetiana Dontsova***: Formal analysis, Supervision.

References

1. Serhiienko, A. O., Dontsova, T. A., Yanushevska, O. I., Nahirniak, S. V., Ahmad, H.-B. (2020). Ceramic membranes: new trends and prospects (short review). Water and water purification technologies. *Scientific and Technical News, 27 (2),* 4–31. https://doi.org/10.20535/2218-93002722020208817
2. Gao, Y., Hao, W., Xu, G., Wang, C., Gu, X., Zhao, P. (2022). Enhancement of superhydrophilic/underwater super-oleophobic performance of ceramic membrane with TiO_2 nanowire array prepared via low temperature oxidation. *Ceramics International, 48 (7),* 9426–9433. https://doi.org/10.1016/j.ceramint.2021.12.139
3. Molchan, Y., Bohdan, L., Kyrii, S., Tymoshenko, O., Pylypenko, I., Burmak, A. et al. (2025). Low-cost ceramic membrane supports based on Ukrainian kaolin and saponite. *Functional Materials, 32 (1),* 87–96. https://doi.org/10.15407/fm32.01.87
4. Yanushevska, O. I., Dontsova, T. A., Aleksyk, A. I., Vlasenko, N. V., Didenko, O. Z., Nypadymka, A. S. (2020). Surface and Structural Properties of Clay Materials Based on Natural Saponite. *Clays and Clay Minerals, 68 (5),* 465–475. https://doi.org/10.1007/s42860-020-00088-4
5. Erdem, I. (2017). Sol-gel applications for ceramic membrane preparation. *AIP Conference Proceedings, 1809,* 020011. https://doi.org/10.1063/1.4975426
6. Vovk, O. F., Davydova, M. Y., Yanushevska, O. I., Kyrii, S. O., Linovytska, V. M., Lapinskyi, A. V., Dontsova, T. A. (2024). Antibacterial properties of ceramic membranes with TiO_2 selective layer. *Journal of Chemical Technology, 32* (2), 351–362. https://doi.org/10.15421/jchemtech.v32i2.298738
7. Benrezgua, E., Deghfel, B., Zoukel, A., Basirun, W. J., Amari, R., Boukhari, A. et al. (2022). Synthesis and properties of copper doped zinc oxide thin films by sol-gel, spin coating and dipping: A characterization review. *Journal of Molecular Structure, 1267,* 133639. https://doi.org/10.1016/j.molstruc.2022.133639
8. Marzouk, S. S., Naddeo, V., Banat, F., Hasan, S. W. (2021). Preparation of TiO_2/SiO_2 ceramic membranes via dip coating for the treatment of produced water. *Chemosphere, 273,* 129684. https://doi.org/10.1016/j.chemosphere.2021.129684
9. Zeribi, F., Attaf, A., Derbali, A., Saidi, H., Benmebrouk, L., Aida, M. S. et al. (2022). Dependence of the Physical Properties of Titanium Dioxide (TiO_2) Thin Films Grown by Sol-Gel (Spin-Coating) Process on Thickness. *ECS Journal of Solid State Science and Technology, 11 (2),* 023003. https://doi.org/10.1149/2162-8777/ac5168
10. Lukong, V. T., Ukoba, K. O., Jen, T. C. (2022). Heat-assisted sol-gel synthesis of tio_2 nanoparticles structural, morphological and optical analysis for self-cleaning application. *Journal of King Saud University – Science, 34 (1),* 101746. https://doi.org/10.1016/j.jksus.2021.101746
11. Al Amin, S. M., Kowser, Md. A. (2024). Influence of Ag doping on structural, morphological, and optical characteristics of sol-gel spin-coated TiO_2 thin films. *Heliyon, 10 (18),* e37558. https://doi.org/10.1016/j.heliyon.2024.e37558
12. Bhandarkar, S. A., Prathvi, Kompa, A., Murari, M. S., Kekuda, D., Mohan, R. K. (2021). Investigation of structural and optical properties of spin coated TiO_2:Mn thin films. *Optical Materials, 118,* 111254. https://doi.org/10.1016/j.optmat.2021.111254
13. Prathvi, Bhandarkar, S. A., Kompa, A., Kekuda, D., S, M. M., Telenkov, M. P., Nagaraja, K. K., Mohan Rao, K. (2021). Spectroscopic, structural and morphological properties of spin coated Zn:TiO_2 thin films. *Surfaces and Interfaces, 23,* 100910. https://doi.org/10.1016/j.surfin.2020.100910
14. Prasad, A., Singh, F., Dhuliya, V., Purohit, L. P., Ramola, R. C. (2024). Structural and optical characteristics of Cr-doped TiO_2 thin films synthesized by sol-gel method. *Optical Materials, 151,* 115411. https://doi.org/10.1016/j.optmat.2024.115411
15. Caligulu, U., Darcan, N., Kejanli, H. (2021). Surface morphology and optical properties of Ca and Mn doped TiO_2 nano-structured thin films. *Engineering Science and Technology, an International Journal, 24 (6),* 1292–1300. https://doi.org/10.1016/j.jestch.2021.05.006
16. Pérez-Jiménez, L. E., Solis-Cortazar, J. C., Rojas-Blanco, L., Perez-Hernandez, G., Martinez, O. S., Palomera, R. C. et al. (2019). Enhancement of optoelectronic properties of TiO_2 films containing Pt nanoparticles. *Results in Physics, 12,* 1680–1685. https://doi.org/10.1016/j.rinp.2019.01.046
17. Baqiah, H., Mustafa Awang Kechik, M., Pasupuleti, J., Zhang, N., Mohammed Al-Hada, N., Fat Chau, C. et al. (2023). Nanostructure, optical, electronic, photoluminescence and magnetic properties of Co-doped ZrO_2 sol-gel films. *Results in Physics, 55,* 107194. https://doi.org/10.1016/j.rinp.2023.107194
18. Mathew Simon, S., George, G., Sajna, M. S., Prakashan, V. P., Anna Jose, T., Vasudevan, P. et al. (2021). Recent advancements in multifunctional applications of sol-gel derived polymer incorporated TiO_2-ZrO_2 composite coatings: A comprehensive review. *Applied Surface Science Advances, 6,* 100173. https://doi.org/10.1016/j.apsadv.2021.100173
19. Ali, M. M., Haque, Md. J., Kabir, M. H., Kaiyum, M. A., Rahman, M. S. (2021). Nano synthesis of ZnO–TiO_2 composites by sol-gel method and evaluation of their antibacterial, optical and photocatalytic activities. *Results in Materials, 11,* 100199. https://doi.org/10.1016/j.rinma.2021.100199

ISSN-L 2664-9969; E-ISSN 2706-5448

20. Chi, N., Wang, Y. (2022). Synthesis and application of CuO-TiO_2 hybrid nanostructures as Photocatalytst for degradation of p-nitrophenol in wastewater. *International Journal of Electrochemical Science, 17 (10),* 221061. https://doi.org/10.20964/2022.10.50

21. Gutierrez-Sanchez, C. D., Téllez-Jurado, L., Dorantes-Rosales, H. J. (2024). Synthesis of zirconia nanoparticles by sol-gel. Influence of acidity-basicity on the stability transformation, particle, and crystallite size. *Ceramics International, 50 (11),* 20547–20560. https://doi.org/10.1016/j.ceramint.2024.03.177

22. Shishodia, G., Gupta, S., Pahwa, N., Shishodia, P. K. (2024). ZrO_2 Nanoparticles Synthesized by the Sol-Gel Method: Dependence of Size on pH and Annealing Temperature. *Journal of Electronic Materials, 53 (9),* 5159–5168. https://doi.org/10.1007/s11664-024-11185-8

23. Chen, M., Heijman, S. G. J., Rietveld, L. C. (2021). State-of-the-Art Ceramic Membranes for Oily Wastewater Treatment: Modification and Application. *Membranes, 11 (11),* 888. https://doi.org/10.3390/membranes11110888

24. Cai, Y., Wang, Y., Chen, X., Qiu, M., Fan, Y. (2015). Modified colloidal sol-gel process for fabrication of titania nanofiltration membranes with organic additives. *Journal of Membrane Science, 476,* 432–441. https://doi.org/10.1016/j.memsci.2014.11.034

25. Schiffer, S., Matyssek, A., Hartinger, M., Bolduan, P., Mund, P., Kulozik, U. (2021). Effects of selective layer properties of ceramic multi-channel microfiltration membranes on the milk protein fractionation. *Separation and Purification Technology, 259,* 118050. https://doi.org/10.1016/j.seppur.2020.118050

26. Molchan, Y., Vorobyova, V., Vasyliev, G., Pylypenko, I., Shtyka, O., Maniecki, T., Dontsova, T. (2024). Physicochemical and antibacterial properties of ceramic membranes based on silicon carbide. *Chemical Papers, 78 (16),* 8659–8672. https://doi.org/10.1007/s11696-024-03695-w

27. Fedenko, Y. M., Dontsova, T. A., Astrelin, I. M. (2012). Turbidymetrychnyi metod otsinky rozmiriv nanochastynok u "bilykh zoliakh" ZrO_2. *Scientific news of NTUU "KPI", 1,* 155–158. Available at: https://ela.kpi.ua/server/api/core/bitstreams/769d2666-ee3f-478d-9aa1-ba83db3a4453/content

28. Kurylenko, V. S., Tereshkov, M. V., Fedenko, Yu. M., Lapinskyi, A. V., Yanushevska, O. I., Dontsova, T. A. (2025). Prospects of using DLP 3D printing technology to produce membrane ceramic modules. *Journal of Chemical Technology, 33* (2), 508–518. https://doi.org/10.15421/jchemtech.v33i2.317663

29. Dixit, C. K., Bhakta, S., Kumar, A., Suib, S. L., Rusling, J. F. (2016). Fast nucleation for silica nanoparticle synthesis using a sol-gel method. *Nanoscale, 8 (47),* 19662–19667. https://doi.org/10.1039/c6nr07568a

30. Chang, C., Rad, S., Gan, L., Li, Z., Dai, J., Shahab, A. (2023). Review of the sol-gel method in preparing nano TiO_2 for advanced oxidation process. *Nanotechnology Reviews, 12 (1).* https://doi.org/10.1515/ntrev-2023-0150

31. Takada, T. (2020). Removal of F- from Water Using Templated Mesoporous Carbon Modified with Hydrated Zirconium Oxide. *C – Journal of Carbon Research, 6 (1),* 13. https://doi.org/10.3390/c6010013

32. Pylypenko, M. M., Yanko, T. B., Stadnik, Y. S., Drobyshevska, A. O. (2019). Processing substandard materials of magnesium-thermal zirconium production. *Problems of Atomic Science and Technology,* 5, 135–141. Available at: https://nasplib.isofts.kiev.ua/handle/123456789/195204

33. Omar, M. F., Ismail, Abd. K., Sumpono, I., Alim, E. A., Nawi, M. N., Rahim Mukri, M. A. (2012). FTIR Spectroscopy Characterization of Si-C bonding in SiC Thin Film prepared at Room Temperature by Conventional 13.56 MHz RF PECVD. *Malaysian Journal of Fundamental and Applied Sciences, 8 (4),* 242–244. https://doi.org/10.11113/mjfas.v8n4.156

34. Zakirov, M., Korotchenkov, O., Rybak, Ya. (2016). Photoluminescence of ZnS Luminophore Sonofragmentated in Isopropyl Alcohol Solution. *Journal of Nano- and Electronic Physics, 8 (4 (1)).* https://doi.org/10.21272/jnep.8(4(1)).04002

35. Al-Amin, M., Dey, S. C., Rashid, T. U., Ashaduzzaman, M., Shamsuddin, S. M. (2016). Solar assisted photocatalytic degradation of reactive azo dyes in presence of anatase titanium dioxide. *International Journal of Latest Research in Engineering and Technology, 2 (3),* 14–21. Available at: https://www.researchgate.net/publication/299441386_Solar_Assisted_Photocatalytic_Degradation_of_Reactive_Azo_Dyes_in_Presence_of_Anatase_Titanium_Dioxide

36. Chougala, L. S., Yatnatti, M. S., Linganagoudar, R. K., Kamble, R. R., Kadadevarmath, J. S. (2017). A Simple Approach on Synthesis of TiO_2 Nanoparticles and its Application in dye Sensitized Solar Cells. *Journal of Nano- and Electronic Physics, 9 (4).* https://doi.org/10.21272/jnep.9(4).04005

37. Ramachandran, M., Subadevi, R., Rajkumar, P., Muthupradeepa, R., Yuvakkumar, R., Sivakumar, M. (2021). Upshot of Concentration of Zirconium (IV) Oxynitrate Hexa Hydrate on Preparation and Analyses of Zirconium Oxide (ZrO_2) Nanoparticles by Modified Co-Precipitation Method. *Journal of Nanoscience and Nanotechnology, 21 (11),* 5707–5713. https://doi.org/10.1166/jnn.2021.19488

✉ ***Liudmyla Bohdan,*** *PhD Student, Department of Inorganic Substances, Water Treatment and General Chemical Technology, National Technical University of Ukraine "Igor Sikorsky Kyiv Polytechnic Institute", Kyiv, Ukraine, ORCID: https://orcid.org/0009-0006-5207-7781, e-mail: bohdan.liudmyla@lll.kpi.ua*

Khrystyna Hutsul, *PhD, Assistant, Department of Inorganic Substances, Water Treatment and General Chemical Technology, National Technical University of Ukraine "Igor Sikorsky Kyiv Polytechnic Institute", Kyiv, Ukraine, ORCID: https://orcid.org/0000-0002-4760-3605*

Olena Yanushevska, *PhD, Associate Professor, Department of Inorganic Substances, Water Treatment and General Chemical Technology, National Technical University of Ukraine "Igor Sikorsky Kyiv Polytechnic Institute", Kyiv, Ukraine, ORCID: https://orcid.org/0000-0002-3457-8965*

Yurii Fedenko, *PhD, Senior Lecturer, Department of Technology of Inorganic Substances, Water Treatment and General Chemical Technology, National Technical University of Ukraine "Igor Sikorsky Kyiv Polytechnic Institute", Kyiv, Ukraine, ORCID: https://orcid.org/0000-0002-8599-1717*

Tetiana Dontsova, *Doctor of Technical Sciences, Professor, Head of Department of Technology of Inorganic Substances, Water Treatment and General Chemical Technology, National Technical University of Ukraine "Igor Sikorsky Kyiv Polytechnic Institute", Kyiv, Ukraine, ORCID: https://orcid.org/0000-0001-8189-8665*

✉ *Corresponding author*